INL/CON-08-14466
PREPRINT

Computational Assessment of the GT-MHR Graphite Core Support Structural Integrity in Air-Ingress Accident Condition

7th International Topical Meeting on Nuclear Reactor Thermal Hydraulics, Operation and Safety

Jong B. Lim
Eung S. Kim
Chang H. Oh
Richard R. Schultz
David A. Petti

October 2008

Computational Assessment of the GT-MHR Graphite Core Support Structural Integrity in Air-Ingress Accident Condition

Jong B. Lim**, Eung S. Kim, Chang H. Oh*, Richard R. Schultz, and David A. Petti
Idaho National Laboratory
P.O. Box 1625
Idaho Falls, ID. 83415
*Chang.Oh@inl.gov

Abstract

The objective of this project was to perform stress analysis for graphite support structures of the General Atomics' 600 MWth Gas Turbine – Modular Helium Reactor (GT-MHR) [1] prismatic core design using ABAQUS ® (ver. 6.75)[2] to assess their structural integrity in air-ingress accident conditions where the structure weakens over time because of oxidation damages. The graphite support structures of prismatic type GT-MHR was analyzed based on the change of temperature, burn-off and corrosion depth during the accident period predicted by GAMMA, a multi-dimensional gas multi-component mixture analysis code developed in the Republic of Korea (ROK)/United States International Nuclear Engineering Research Initiative (US I-NERI) project [3]. Both the load and thermal stresses were analyzed, but the thermal stress was not significant, leaving the load stress from weight of the core to be the major factor. The mechanical strengths are exceeded between 11 to 11.5 days after the loss-of-coolant-accident (LOCA), corresponding to 5.5 to 6 days after the start of natural convection.

** Summer student from the University of Wisconsin-Madison

Keywords

GT-MHR, Graphite Oxidation, GAMMA, Stress Analysis

1. INTRODUCTION

The Very High Temperature Reactor (VHTR) is one of favored concepts among the designs proposed for the Next Generation Nuclear Plant (NGNP) because of its inherent safety against LOCA and efficient hydrogen production capability. However, the inherent safety feature of the VHTR graphite core design could be compromised if the core support structures collapse and damage the fuel blocks, potentially leading to release of fission products. Such a failure could eventually occur in air-ingress accident, where the graphite support structures are gradually damaged over time because of oxidation, altering their shapes and mechanical properties. To determine the time scale of the graphite support structure failure, computational stress analysis was performed with ABAQUS (ver. 6.75) using the transient corrosion depth, temperature and burn-off predicted by the GAMMA.

2. SUPPORT STRUCTURE STRESS ANALYSIS STRATEGY AND DIMENSIONS

The core is made of several layers of graphite blocks. To finish the computational analysis in a reasonable amount of time, instead of modeling the entire core, only one vertical column of the support block and plenum directly below fuel blocks, the parts subjected to most stress and oxidation damage, was analyzed.

The support block is a hexagon, 36 cm in diameter and 79.4 cm in height, with 1.88 cm triangular pitched coolant channels (102 channels with 1.58 cm diameter and 6 channels with 1.27 cm diameter), and it is modeled using the dimensions of General Atomics' GT-MHR fuel block design [1, 4, 5]. The dimensions used for modeling the plenum are based on the order of magnitude estimates for geometric ratios suitable for normal operation of a 600 MWth GT-MHR [6]. The plenum is approximately 316 cm tall and coolant channels converge into six jet holes located in corners of the hexagon located 30 cm below the plenum's top. The information on how the coolant channels converge into the jet hole was not available; therefore they were assumed to be designed using rotational symmetry such that equal number of channels converges into each jet holes.

3. CHANGE OF TEMPERATURE, BURN-OFF & CORROSION THICKNESS

In order to analyze the core temperature, graphite oxidation, and corrosion, GAMMA code has been used [2]. In this modeling, helium at 490 ^{o}C and 7 MPa initially enters the prismatic core through the riser and exits at 850^{o}C. The initial flow rate was assumed to be 320 kg/s. For conservative analysis, the volume of the containment was assumed to be infinitely large (= 1×10^{6} m^{3}). All the core support was assumed to be graphite materials. The graphs in the Fig. 1, 2 and 3 show the GAMMA results for transient corrosion depth, temperature, and burn-off for sections of the support block and plenum. Corrosion refers to oxidation taking place on the outer surfaces of the structure exposed to airflow. Burn-off refers to the oxidation of the graphite's internal body, causing reduction of density, Young's modulus and mechanical strengths. As shown in Fig. 2 and 3, the temperature and burn-off start to rise at about 5.5 days after the LOCA, and this is the time when the natural convection starts. The heat from exothermic oxidation reaction causes the temperature to

rise, and increased temperature also increases the oxidation rate. The temperature and availability of oxygen plays key roles in oxidation damage. Corrosion and burn-off are the highest on the section 6 because of high temperature. Corrosion and burn-off are not as high above the section 6 because of depletion of oxygen.

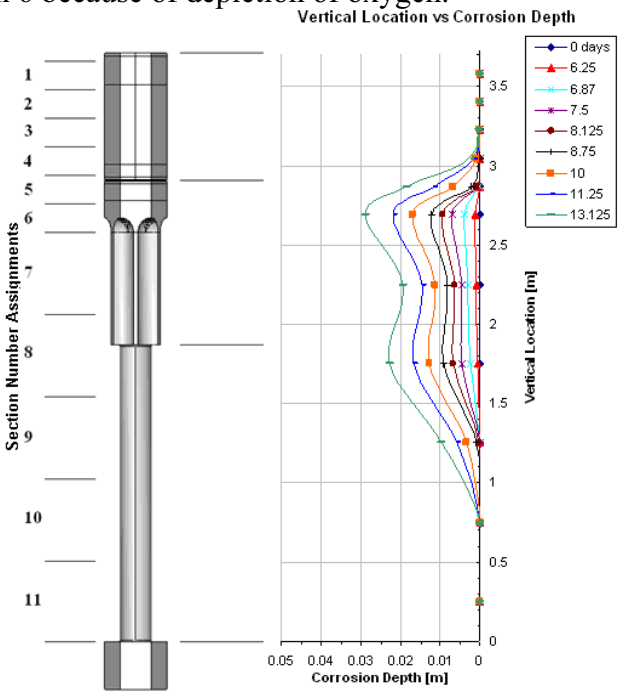

Fig. 1. Corrosion depths and section assignments from GAMMA calculations.

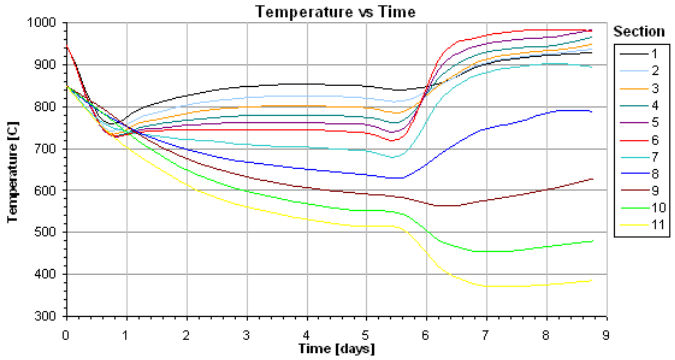

Fig. 2. Temperature over time for each section from GAMMA calculations.

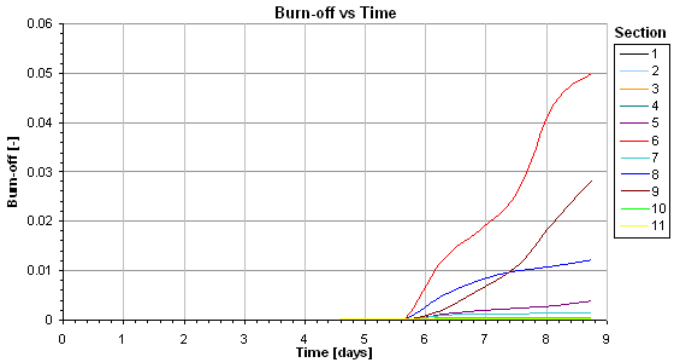

Fig. 3. Burn-off over time for each section from GAMMA calculations.

4. MATERIAL DATABASE

IG-110, one of candidate graphites for the VHTR [7], was used for the stress analysis. Mechanical properties and strengths are important for accuracy of the analysis, therefore a detailed material database was built to address properties and strengths in standard conditions [8, 9] as well as the effects of the temperature [10], burn-off [8,10], and irradiation [11, 12]. The burn-off was found to be the most important factor affecting properties and strengths. The change of mechanical properties from the irradiation is expected to be negligible because of low neutron dose experienced by the support block and plenum.

5. TREATMENT OF MATERIAL PROPERTIES DURING ANALYSIS

The IG-110 is treated as an ideal brittle material, which exhibits elastic behavior with a constant Young's modulus and does not undergo any plastic deformation before reaching the strength limit. This approximation is applicable to IG-110 because IG-110 is a brittle ceramic material that undergoes negligible plastic deformation before failure.

During the analysis, the Young's modulus and density were estimated for the respective temperature and burn-off of the time and section number shown in the Fig. 2, and 3, respectively. For this report, the principal stress failure criterion is used as failure criteria. The failure is assumed occur if the minimum principal stress (maximum compressive stress) exceeds the ultimate compressive strength, or if the maximum principal stress (maximum tensile stress) exceeds the ultimate tensile strength.

6. INITIAL PRE-OXIDIZED STATE RESULTS

6.1. Pre-Oxidized State Load Stress

As the first step, the support block and plenum in pre-oxidized condition was analyzed to understand general stress distribution. The Fig. 4 shows the maximum compressive stress distribution on the support block and plenum in pre-oxidized condition, analyzed using 1/6

cyclic symmetry. The Fig. 4a, 4b, 4c, and 4d show the zoomed up views of the support block top, support block middle, plenum top, and plenum bottom, respectively with the meshing removed for better views of the stress distributions. As shown in the Fig. 4d, the maximum stress is concentrated on the root of the plenum, indicated in red color, which corresponds to 1 MPa, far below the mechanical strength limit of undamaged IG-110, which is 61.3 MPa [8]. Although not shown on the figure, the maximum tensile stress is 0.1 MPa, again far below the tensile strength limit, which is 19.4 MPa [8]. Because the corrosion and burn-off on lower part of the plenum and upper part of the support block are negligible, stress distribution on these parts would be about the same on other time points, and it is unnecessary to include them in analysis, therefore only the part within point L1 to L2, indicated in the Fig. 4, was analyzed to reduce size of the model and computation time.

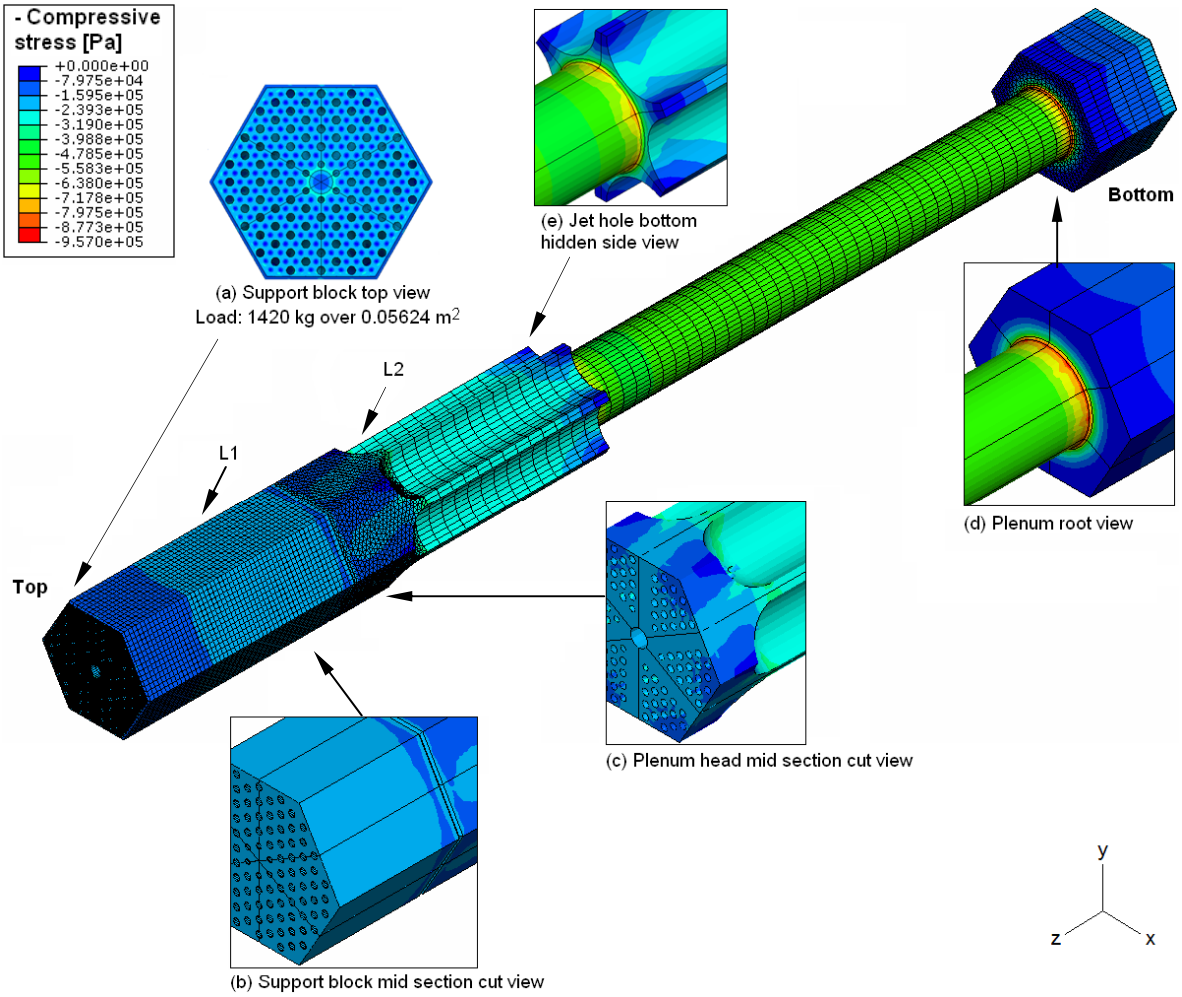

Fig. 4. Compressive stress distribution on pre-oxidized support block and plenum.

6.2. Pre-Oxidized State Thermal Stress

Thermal stress analysis was done for a small representative part of the support block including three coolant channels. The temperature difference between the outer surface and

the inner body is expected to be in order of couple tens of degrees at most, therefore the coolant channel surface temperature of 1300K and internal body temperature of 1250K were assumed. The maximum compressive and tensile stresses are 1.74 MPa and 1.71 MPa, respectively, far below the maximum compressive and tensile strength limits.

7. OXIDIZED STATE RESULTS

7.1. Oxidized State Model

For oxidized states, simple modifications were made to the height of the plenum head section and support block to make them more structurally sound. Stress concentration would occur at the contact surface between the support block and plenum head, and this is primarily because of the chamfer feature, which significantly reduces the size of cross sectional area available to support the load in heavily corroded state. The structure could last longer if the interacting surface is relocated to some other place where oxidation damage is negligible, and this is accomplished by adjusting the height of the plenum head and the support block by 24 cm. The Fig. 5 shows 1/6 cyclic symmetry unit of the modified plenum head for particular times during transient. As corrosion progresses and the coolant holes collapse together, the plenum head eventually develops pillars, remains of the thickest parts of the plenum head. The table 1 shows the material properties used for each day.

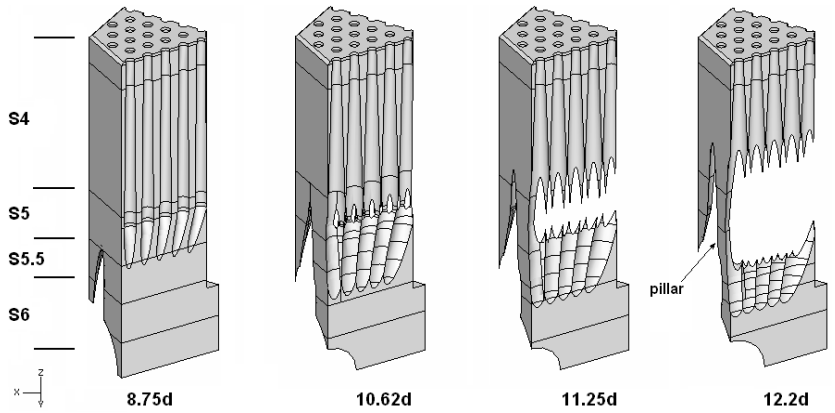

Fig. 5. Assumed 1/6 cyclic symmetry units of the modified plenum head for each day.

Table 1. Material properties at each day.

Day	S	T [K]	burnoff [-]	Density [kg/m3]	Young's Modulus [GPa]	Compressive strength [MPa]	Tensile strength [MPa]
8.75	4	950	0.000	1780	8.68		
	5	980	0.028	1730	6.98		
	5.5	980	0.039	1710	6.38		
	6	980	0.050	1691	5.83	43.5	13.8
10.62	4	950	0.000	1780	8.68		
	5	980	0.007	1768	8.27		
	5.5	980	0.043	1703	6.16		
	6	980	0.080	1638	4.53	35.5	11.2
11.25	4	950	0.000	1780	8.68		
	5	980	0.010	1762	8.07		
	5.5	980	0.050	1691	5.84		
	6	980	0.090	1620	4.16	33.2	10.5
12.25	4	950	0.000	1780	8.68		
	5	980	0.015	1754	7.77		
	5.5	980	0.060	1673	5.35		
	6	980	0.106	1592	3.62	29.8	9.4

7.2. Oxidized State Load Stress

The Fig. 6a and 6b show maximum compressive and tensile stresses for two different locations, the 'edge' and 'inside', indicated in the Fig. 7b and 7c for compressive stress and the Fig. 8b and 8c for tensile stress. The support structure starts to take significant oxidation damage when the natural convection starts to occur, which is 5.5 days after LOCA. The stress concentrations are increasing almost exponentially over time because they are inversely proportional to the cross sectional area, which is also decreasing over time because of corrosion. From observing the Fig. 7a and 7b, it can be seen that the bottom half of the pillar is slanted to left, and this creates counter clockwise bending moment, causing compressive stress (Fig. 7b) toward left side and tensile stress (Fig. 8b) toward right side. On the other hand, the top half of the pillar is straight, and because of the counter clockwise bending moment of the bottom half, the top half of the pillar is subjected to compressive stress on the right side and tensile stress on the left side. Local maximum near the edge occurs because the bending moment causes the greatest stress on the outer edge, and the stress concentration on the edge gets exacerbated by decreasing cross sectional area toward the edge because of the triangular shape. The stress is relieved toward the inner section where cross sectional area gets relatively larger. It is to be noted that exceeding strength limit on the edge do not necessarily lead to failure, because after edge portion crumbles, the stress will get redistributed to inner section, and inner section's cross sectional area is most likely wide enough to handle the additional loading without much change in stress concentration. On the other hand, exceeding mechanical strength on inner section is a

definite sign of failure because failure in inner section results in significant loss of cross sectional area to handle the load.

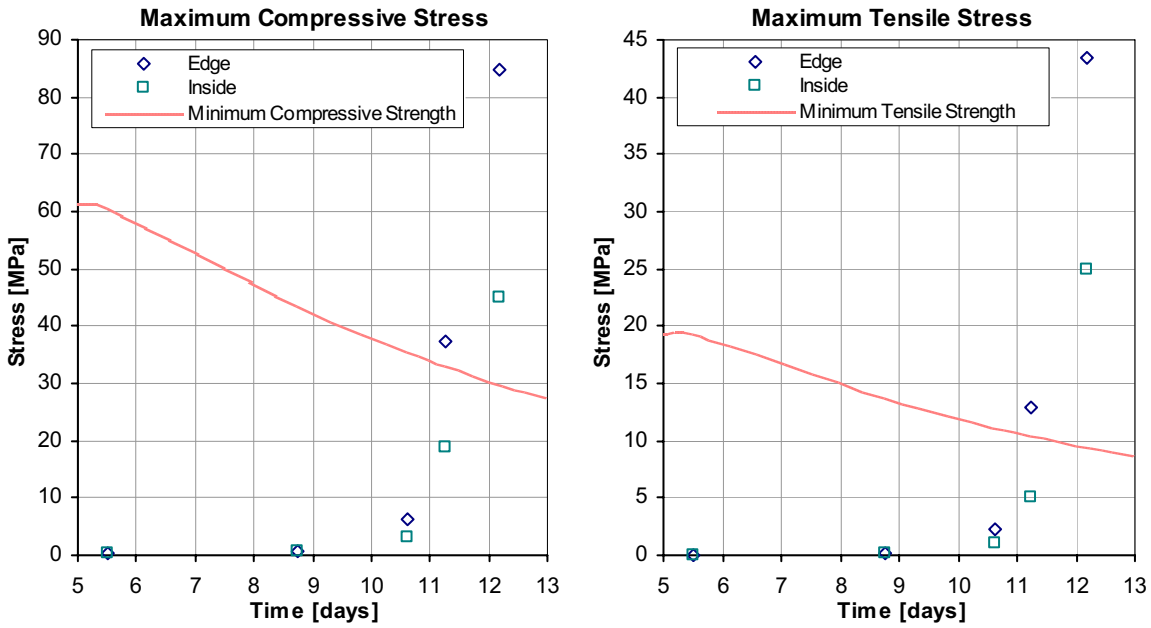

(a) **(b)**

Fig. 6. Maximum compressive stress (a) and tensile stress (b) over time.

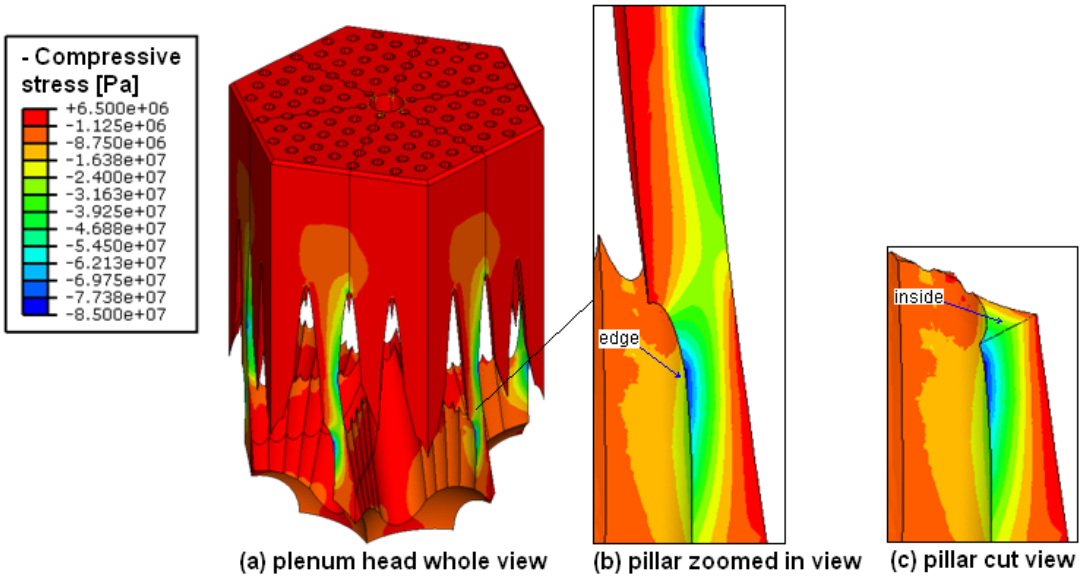

Fig. 7. 1/6 geometry repeated whole view of the compressive stress distribution on plenum head, 12.25 days after LOCA.

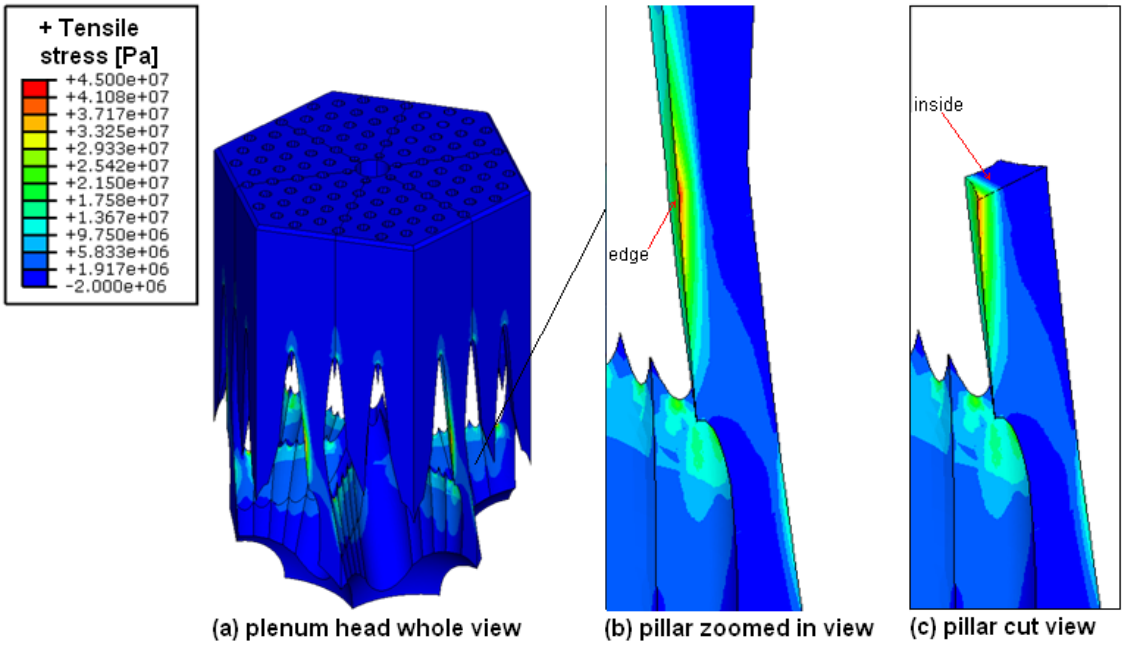

Fig. 8. 1/6 geometry repeated whole view of the tensile stress distribution on plenum head, 12.25 days after LOCA.

7.3. Oxidized State Thermal Stress

Just like the pre-oxidized case, the thermal stresses in the oxidized case are negligible. Thermal stress analysis for oxidized state model was performed for small portion of the 11.25 day model's surviving pillar. The temperature was set to 1350 K for the inner surface exposed to air flow, and 1300 K for the outer surface not exposed to air flow. As shown in the table 2, compared to the stress caused by the load alone, thermal stress is an order of magnitude smaller. Slight stress reduction in combined load case could be caused by increase in size of the cross sectional area from thermal expansion.

Table. 2 Comparison of thermal and load stresses on an oxidized pillar.

	Compressive stress [MPa]	Tensile stress [MPa]
Thermal stress only (1300 – 1350 K)	1.17	0.83
Load stress only	46.62	8.234
Both thermal and load stresses	46.49	8.123

8. CONCLUSION AND FURTHER RESEARCH

The graphite support structures of prismatic type GT-MHR was analyzed based on the transient temperature, burn-off and corrosion depth during the accident period predicted by GAMMA. The greatest stress concentration occurs on the plenum head section, which experiences the most corrosion and burn-off damages. The stress concentration increases

over time because of corrosion, which reduces the size of the plenum head's cross sectional area to support the load. Also, the mechanical strengths decrease over time because of internal burn-off. The mechanical strengths are exceeded between 11 to 11.5 days after LOCA, corresponding to 5.5 to 6 days after the start of natural convection.

According to a new air ingress study using FLUENT, which accounted for the density-gradient driven stratified flow and molecular diffusion, the natural convection could occur a lot sooner than GAMMA code's prediction, which excluded the density-gradient phenomenon [13]. This could affect the transient temperature, corrosion and burn-off profiles, which would also affect the stress analysis, therefore further investigations are needed to update the transient data used for stress analysis.

It may be possible to avoid the support structure failure from oxidation damage by supplementing it with independent structures that are oxidation resistant and able to support the core on its own. One such a structure would be a large plate spanning across the core in horizontal plane right below the fuel block, acting as a floor to the fuel blocks, supported by posts placed in center of each fuel column though the graphite support block and plenum. The plate and the posts will have to be made of high temperature refractory material that is resistant to oxidation or can be coated to protect it against oxidation. The graphite support block and plenum will need to be still present to take the oxidation damage and thus prevent oxygen from reaching the fuel blocks. If possible, using oxidation resistant independent structure could eliminate the concern for support structure failure from oxidation damage; therefore it would be worth a while to investigate potential independent support structure design.

ACKNOWLEDGEMENTS

This work was supported through the Department of Energy's ROK/US I-NERI (Project number of 2007-001-K) under DOE Idaho Operations Office Contract DE-AC07-99ID13727.

REFERENCES

1. General Atomics, *International GT-MHR Project Internal Design Review Presentation Material*, San Diego, December 8-12, 1997.
2. ABAQUS, Inc., ABAQUS 6.75 Analysis User's Manual, 2007.
3. C. H. Oh, C. Davis, L. Siefken, R. Moore, H. C. No, J. Kim, G. C. Park, J. C. Lee, W. R. Martin, *Development of Safety Analysis Codes and Experimental Validation for a Very High Temperature Gas-Cooled Reactor*, INL/EXT-06-01362, March 2006.
4. F.G. Cocheme, *Assessment of Passive Decay Heat Removal in the General Atomic Modular Helium Reactor*. Master's thesis, Texas A&M University, Texas, 2004.
5. General Atomics, *Screening Tests for Selection of VHTR Advanced Fuel*, Contract No. DE-AC03-01SF22343, Revision 0, 2003.

6. G.E. McCreery, D.M. McEligot, *Scaling Studies and Conceptual Experiment Designs for NGNP CFD Assessment*, INEEL/EXT-04-02502, November 2004.
7. T. Shibata, T. Tada, J. Sumita, K. Sawa, "Oxidation Damage Evaluation by Non-Destructive Method for Graphite Components in High Temperature Gas-Cooled Reactor", *Journal of Solid Mechanics and Materials Engineering*, Vol. 2, No. 1 (2008), pp.166-175 .
8. M. Ishihara, T. Iyoku, T. Oku, T. Shibata, J. Sumita, "Principle Design and Data of Graphite Components," *Nuclear Engineering and Design*, Vol. 233, pp. 251-260., 2004.
9. T.D. Burchell, G.R. Romanoski, *The Effects of Specimen Geometry and Size on the Fracture Toughness of Nuclear Graphites*, ORNL CONF-9109266-1, January 1991.
10. M. Eto, T. Konishi, T. Oku, "High Temperature Young's Modulus of IG-110 Graphite," JAERI, Conference article from Specialists' meeting on graphite component structural design, JAERI Tokai (Japan), September 8-11, 1986, conducted by the International Atomic Energy Agency, Vienna (Austria). International Working Group on Gas-Cooled Reactors. IWGGCR—11, pp. 133-137., 1986.
11. T.D. Burchell, M. Eto, S. Ishiyama, J.P. Strizak, "The Effect of high Fluence Neutron Irradiation on the Properties of a Fine-Grained Isotropic Nuclear Graphite," *Journal of Nuclear Materials*, 230, pp. 1-7., 1996.
12. G.O. Hayner, W.R. Corwin, R.L. Bratton, T.D. Burchell, R.N. Wright, J.W. Klett, W.E. Windes, R.K. Nanstad, T.C. Totemeie,r L.L. Snead, K.A. Moore, Y. Katoh, P.L. Rittenhouse, R.W. Swindeman, D.F. Wilson, T.D. McGreevy, *Next Generation Nuclear Plant Materials Research and Development Program Plan*, INL/EXT-05-00758 Rev. 2, September 2005.
13. C. H. Oh, E. S. Kim, R. Schultz, D. Petti, "Implication of Air Ingress Induced by Density-Difference Driven Stratified Flow," *ICAPP'08*, paper no. 8023, Anaheim, CA, June 8-12, 2008.